

Cortical Mapping of Magnetic Susceptibility and R2* reveals Insights into Tissue Composition

Andreas Deistung¹, Andreas Schäfer², Ferdinand Schweser^{3,4}, and Jürgen Rainer Reichenbach¹

¹Medical Physics Group, Institute of Diagnostic and Interventional Radiology, Jena University Hospital - Friedrich Schiller University Jena, Jena, Germany,

²Department of Neurophysics, Max-Planck-Institute for Human Cognitive and Brain Sciences, Leipzig, Germany, ³Buffalo Neuroimaging Analysis Center, Dept. of Neurology, School of Medicine and Biomedical Sciences, State University of New York at Buffalo, Buffalo, NY, United States, ⁴MRI Molecular and Translational Imaging Center Institution, Buffalo CTSC, State University of New York at Buffalo, Buffalo, NY, United States

TARGET AUDIENCE: Researchers with interest in quantitative susceptibility mapping, relaxometry, and tissue composition of the cerebral cortex.

INTRODUCTION: Non-invasive assessment of the tissue composition of the cerebral cortex is important for comparing results across functional magnetic resonance imaging (fMRI) studies. Thus, cortical mapping of the MRI signal has previously been proposed to study anatomical features in the cerebral cortex *in vivo*.^{1,2} Gradient-echo (GRE) imaging allows assessing the human brain anatomy in high-spatial resolution^{3,4} and determining two quantitative physical properties, the effective transverse relaxation rate (R_2^*) and the magnetic susceptibility (χ) of the bulk tissue.^{5,6} Interestingly, while both magnetic susceptibility and R_2^* increase linearly with the concentration of paramagnetic iron,^{7,8} the relation is opposed when myelination increases: magnetic susceptibility decreases (becomes more diamagnetic) and R_2^* increases with higher myelination.⁹ Therefore, concomitant analysis of both magnetic susceptibility and R_2^* promises to reveal new insights into the tissue composition *in vivo*.^{10,11} In this contribution, we investigate the spatial distribution of both magnetic susceptibility and R_2^* across the cerebral cortex *in vivo* and assess whether they coincide with the cytoarchitecture.

MATERIAL AND METHODS: *Data Acquisition:* Seven healthy right-handed subjects (3 male and 4 female; 25.3±3.1year) were measured on a 7 T MRI system with a fully flow compensated 3D single-echo gradient-echo sequence (TE/TR/FA = 10.5ms/17ms/8°; BW=140Hz/px, voxel size = (0.4×0.4×0.4) mm³). To enable computation of susceptibility maps using the COSMOS approach¹² the scans were carried out with the head in three different orientations with respect to the magnetic field. In addition, multi-echo 3D GRE imaging (TE₁₋₄ = 5ms/12.8ms/20.6ms/28.4ms, TR/FA = 34ms/8°, BW=160Hz/px, voxel size = (0.8×0.8×0.8) mm³) was carried out with normal head orientation to compute quantitative R_2^* maps. Finally, 3D, whole-head, T₁-weighted MRI data were collected at 3T with an MP-RAGE sequence (TE/TR/TI/FA=3.46ms/1300ms/650ms/10°, isotropic voxel size = 1 mm³). The local ethics committee approved the experiments and informed written consent was obtained from each recruited subject. *Data Processing:* The complex-valued GRE data acquired in tilted head positions were non-linearly registered to the data acquired in normal head position. Phase aliasing was resolved by 3D phase unwrapping¹³ and background phase contributions were eliminated with the SHARP technique.⁵ From the three background field corrected phase data sets susceptibility maps were computed using the COSMOS algorithm^{5,12} and referenced with respect to frontal deep white matter (WM).⁴ Maps of the effective transverse relaxation rate were computed from the multi-echo GRE data using logarithmic calculus. *Data Analysis:* To analyze the distribution of magnetic susceptibility and R_2^* across cortical gray matter (GM) a surface-based analysis approach was applied. To this end, subject-specific cortical surfaces (white matter surface, pial surface) were generated by Freesurfer's automatic processing of T₁-weighted data.¹⁴ Magnitude information of both the single-echo GRE data in normal head position and the multi-echo GRE data were registered linearly to the T₁-weighted dataset. The resulting registration matrices were applied for resampling the volumetric data sets of magnetic susceptibility and R_2^* , respectively, along the midline between the pial and white matter surface (70% of depth) across the entire cortical hemisphere. Unreliable values within the cortices were identified, comprising (I) the outer surface regions of the cortex due to the intrinsic limitation of the SHARP phase pre-processing step, (II) voxels with a susceptibility difference exceeding 45 ppb relative to frontal deep WM to avoid contributions of pial vessels in the cortical subregions, and (III) voxels with R_2^* values exceeding 70 s⁻¹ to avoid regions affected by air-tissue or bone-tissue interfaces. The individual surface representations of magnetic susceptibility, R_2^* , and unreliable values were registered to Freesurfer's 'fsaverage' template by spherical registration.¹⁵ Finally, the resampled surface values were averaged over all subjects (with consideration of the unreliable regions), smoothed across the surface using a 1mm FWHM Gaussian kernel, and overlaid onto the inflated cortical white matter surface.

RESULTS: The distribution of magnetic susceptibility (χ) and R_2^* across the cortical GM is illustrated in **Figure 1**. The magnetic susceptibility resembles the subdivision defined by the probabilistic Brodmann atlas with homogeneous regions of increased susceptibility in certain areas such as BA3 (primary somatosensory cortex), BA4 (primary motor cortex), BA19 (associative visual cortex), and BA42 (auditory association cortex). These regions exhibited increased R_2^* values that also coincided with the boundaries determined by the probabilistic Brodmann atlas. Other regions exhibited quite heterogeneous distributions of susceptibility and/or R_2^* , for example, BA6 (premotor cortex), BA24 (ventral anterior cingulate cortex), and BA40 (supramarginal gyrus). Cortical mapping of magnetic susceptibility and R_2^* also revealed noticeable increases in the primary sensorimotor and auditory cortices (see arrows in **Figs. 1A** and **1C**). Increased R_2^* values were also discernible in the occipital cortex (black arrows in **Fig. 1G**). Regions with decreased R_2^* values were noticeable in the frontal and prefrontal cortices (white arrow in **Fig. 1G**). Additionally, a 'strip' pattern of increased susceptibility and R_2^* was observed along the central sulcus (black arrows in **Figs. 1A** and **1C**).

DISCUSSION: Substantial variations of magnetic susceptibility and R_2^* have been observed across the cortical surface. Magnetic susceptibility and R_2^* of certain regions coincided with the boundaries of the probabilistic Brodmann atlas, whereas other regions exhibited a heterogeneous distribution of magnetic susceptibility and R_2^* within the specific Brodmann area. This finding is not surprising because there is not necessarily a direct correspondence between myeloarchitecture and cytoarchitecture.¹⁶ The high values of χ and R_2^* showing a characteristic 'strip' in the motor-sensory area (BA3, BA4) are indicative for a relative high iron concentration. Interestingly, such a 'strip' pattern of increased myelination along the central sulcus has also recently been detected by mapping the ratio of T₁ and T₂ weighted images² suggesting that both iron and myelin are highly co-localized in BA3 and BA4, which has also been demonstrated recently in the visual cortex.¹⁷ In future, the question of co-localization of iron and myelin across the cerebral cortex may be investigated non-invasively by additionally taking into account other quantitative MRI parameters sensitive to myelin, such as magnetization transfer contrast¹⁸ or the longitudinal relaxation rate (R_1).¹⁹

CONCLUSION: Cortical mapping of R_2^* and magnetic susceptibility represents a non-invasive means to assess tissue composition across the cerebral cortex and may be instrumental for understanding the relationship between tissue composition and functional roles of cortical GM.

REFERENCES: [1] Fischl B et al., *NeuroImage*. 2004;23(Suppl. 1): S69–S84. [2] Glasser MF and van Essen DC, *J Neurosci*. 2011;31(32):11597–11616. [3] Deistung A et al., *Magn Reson Med*. 2008;60(5):1155–1168. [4] Deistung A et al., *NeuroImage*. 2013;65:299–314. [5] Schweser F et al., *NeuroImage*. 2011;54(4):2789–807. [6] Cohen-Adad J, *NeuroImage*. 2014;93(Pt2):189–200. [7] Langkammer et al., *Radiology*. 2010;257(2):455–462. [8] Langkammer et al., *NeuroImage*. 2012;62(3), 1593–1599. [9] Langkammer et al., *NeuroImage*. 2012;59(2), 1413–1419. [10] Schweser F et al., *Proc Intl Soc Mag Reson Med*. 2012;20:409. [11] Schweser F et al., *Proc Intl Soc Mag Reson Med*. 2013; 21:460. [12] Liu T et al., *Magn. Reson. Med*. 2009;61(1):196–204. [13] Abdul-Rahman HS et al., *Appl Opt*. 2007;46(26):6623–6635. [14] Fischl B et al., 2002. *Neuron*. 33 (3):341–355. [15] Fischl B et al., *Hum Brain Mapp*. 1999;8(4), 272–284. [16] Geyer S et al., *Front. Hum. Neurosci*. 2011;5:19. [17] Fukunaga M et al., *Proc. Natl. Acad. Sci. U. S. A.* 2010;107(8):3834–3839. [18] Levesque IR et al., *Magn Reson Med*. 2010;63:633–640. [19] Koenig, S.H., *Magn Reson Med* 1991;20(2):285–291.

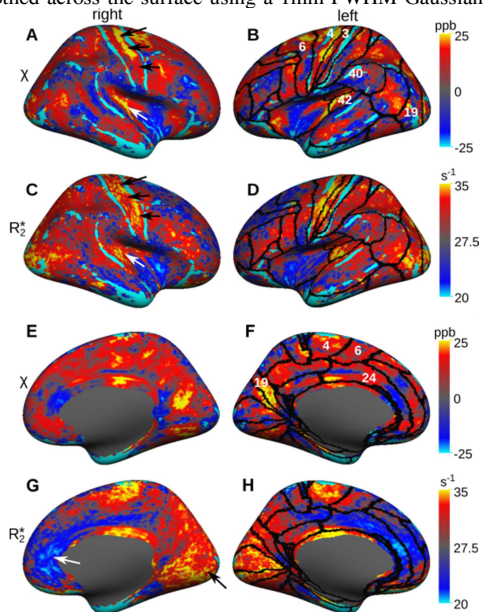


Figure 1: Lateral view (A-D) and medial view (E-H) of the inflated white matter surface with overlays of magnetic susceptibility (A,B,E,F) and R_2^* values (C,D,G,H). The cortical surfaces of the right and left hemispheres are presented in the left and right column, respectively. The black boundaries in the right column indicate the boundaries of the probabilistic Brodmann areas. The numbers denote the corresponding Brodmann area. Regions without reliable susceptibility and R_2^* values are colored cyan, i.e., indicated by $\chi < -25$ ppb and $R_2^* < 20$ s⁻¹.